ASTRONOMY
AND
ASTROPHYSICS

Spectroscopic analysis of the Alpha Centauri system[*,**]

C. Neuforge-Verheecke[***] **and P. Magain** [†]

Institut d'Astrophysique de l'Université de Liège, 5, Avenue de Cointe, B-4000 Liège, Belgium

Received 21 May 1997 / Accepted 24 July 1997

Abstract. A detailed spectroscopic analysis of the two components of the binary system α Centauri has been carried out on the basis of extensive high resolution and high signal-to-noise spectra. The temperatures of the stars have been determined from the Fe I excitation equilibrium and checked from the H_α line wings. The abundances of 17 elements have been obtained and indicate a general overabundance of 0.24 dex relative to the Sun, with no significant difference between the two stars. All elements analysed, from CNO to the iron peak, show basically the same overabundance. Only nickel seems to be significantly more overabundant, while the neutron capture elements appear less enhanced.

Key words: stars: α Centauri – stars: binaries: visual; abundances; fundamental parameters

1. Introduction

The visual binary system α Centauri is the closest system to the Sun. Its parallax and the masses of both components α Cen A and B are known with high accuracy (Demarque et al. 1986).

If precise determinations of the chemical composition and of the effective temperature of both components are available, calibrations of the system can be performed to constrain the theoretical models of these stars (Noels et al. 1991, Fernandes & Neuforge 1995, Neuforge et al. 1997).

Although the α Cen system has already been widely investigated (French and Powell 1971, Bessel 1981, England 1980, Soderblom 1986, Smith et al. 1986, Gratton & Sneden 1987, Abia et al. 1988, Edvardsson 1988, Furenlid & Meylan 1990,

---

Table 1. Determinations of $T_{\rm eff}$ and [Fe/H] for α Cen A and B

Reference	T_A	[Fe/H]$_A$	T_B	[Fe/H]$_B$
FP71	5770	+0.22	5340	+0.12
E80	5750	+0.28	5260	+0.38
B81	5820	-0.01	5350	-0.05
S86	5770	—	5350	—
SEF86	5820	+0.20	5280	+0.20
GS87	5750	+0.11	5250	+0.08
ARCB88	5770	+0.22	5300	+0.14
FM90	5710	+0.12	—	—
CFBG92	5800	+0.22	5325	+0.26
E93	5720	+0.20	—	—
This work	5830	+0.25	5255	+0.24

Meylan et al. 1992, Chmielewski et al. 1992, Edvardsson et al. 1993), no agreement has yet been reached on the precise value of the effective temperatures $T_{\rm eff}$ and of the element abundances in the atmospheres of these stars. Table 1 presents a summary of the determinations of $T_{\rm eff}$ and the iron abundance [Fe/H] in α Cen A and B. It is seen that the proposed values of $T_{\rm eff}$ differ by more than 100 K, while the Fe abundances – excluding the very discrepant determination of Bessell (1981) – vary by some 50%. These uncertainties directly affect the theoretical calibrations and the evolutionary status of the stars. Noels et al. (1991) performed calibrations of the α Cen system using the mixing length formalism of Böhm-Vitense (1958) for the treatment of convection and assumed a unique convection parameter for the two stars. In their analysis, the convection parameter, α, the metallicity of the system, Z, its helium content, Y, and its age, t, are the four unknowns. These unknows are determined by the effective temperatures and the luminosities fitting of the two components of the system. For fixed luminosities, they find that a 100K variation of the effective temperature difference between the two stars lead to a 50 % variation of Z, a 15 % variation of Y, a 10 % variation of α and a 3 % variation of t.

Given this unsatisfactory situation, we decided to perform a detailed and self-consistent determination of the atmospheric parameters and chemical composition of both components of the system, including the CNO abundances. For this purpose, we have obtained a large set of high resolution and high signal-to-noise spectra, forming indeed the best database available for

the two components of this binary system. These data have been reduced and analysed in a very careful way, with the aim of obtaining more accurate and reliable results than was possible with the previously available spectra.

2. Spectroscopic observations

The observations were carried out with the long camera of the Coudé Echelle Spectrometer (CES) fed by the 1.4m Coudé Auxiliary Telescope (CAT) at the European Southern Observatory (La Silla, Chile) and were conducted in remote control from Garching near Munich, during 8 nights, in May 1993.

The detector was a Ford Aerospace CCD (ESO nr. 34, 2048 $\times$ 2048 pixels of 15 μm each). The slit width was adjusted to reach a resolving power of about $100,000$. The exposure times were chosen so that the S/N ratio remains above 400 in each spectral region. Two exposures of each star in each spectral region were taken so that the final S/N ratio reaches ~ 550.

α Cen A and B being solar-type stars, we decided to perform the spectrosopic analysis of the system differentially with respect to the Sun. For this purpose, the solar spectrum was obtained either from the moonlight or from the light reflected by the dome of the 3.60m telescope, depending on the spectral region.

A total of 33 spectral regions were observed, with central wavelengths $\lambda = 5038, 5098, 5150, 5233, 5298, 5380, 5640, 5674, 5708, 5742, 5776, 5810, 5844, 5878, 6010, 6050, 6090, 6130, 6170, 6210, 6250, 6290, 6330, 6370, 6460, 6602, 6642, 6682, 6722, 7468, 7887, 7970$ and 8210 Å.

3. Data reduction and line measurements

The data reductions were carried out with specific procedures written in the ESO-MIDAS environment. Our spectra have been background substracted and flat-fielded in the usual way. The wavelength calibration has been established with the help of the stellar lines themselves.

A critical step in the reduction procedure is the determination of the continuum level. In order to reach the highest accuracy, we selected a number of continuum windows by inspection of the Liège solar atlas (Delbouille et al. 1973). The mean level was computed in each of these windows and a low order spline fitted through these points. The latter was adopted as the continuum level.

The lines used for the spectroscopic analysis were also selected by inspection of the Liège Solar Atlas. We kept only the lines which appear symmetrical and apparently unblended. Possible blends have been estimated with the tables of semi-empirical $\log gf$-values of Kurucz & Peytremann (1975) and the ambiguous cases eliminated. Our selected lines are, as far as possible, located in regions where the continuum windows appearing in the Sun are still present in both components of the α Cen system. The continuum windows are indeed reduced in the two stars since the neutral metal lines are stronger both because of higher metallicity and also of lower effective temperature in the case of α Cen B. For these reasons, most of our spectral
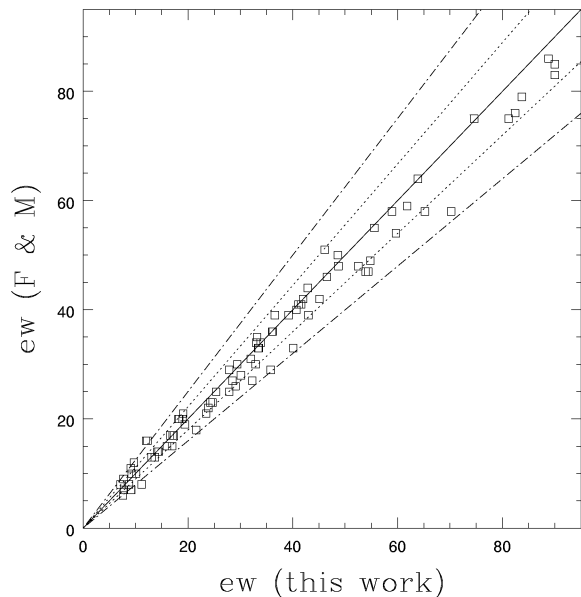

Fig. 1. Comparison between our equivalent width measurements for α Cen A and those of Furenlid & Meylan (1990). Dotted (resp. dot-dashed) lines identify loci where the equivalent widths differ by 10 (resp.) 20 %

regions are centered at longer wavelengths, where fewer lines are present, than those selected by Furenlid & Meylan (1990).

The equivalent width (EW) measurements were made both by direct integration and by least squares fitting of Gaussian and Voigt functions on the observed line profiles (Drayson 1975, Press et al. 1990), the latter allowing to properly take the line wings into account. The final EWs are weighted means of these measurements, the weights being chosen by visual examination of the quality of the fits.

Our selected lines are listed in Table 4. This table gives, for each element in a given ionization state (column 1), the wavelength of the line, its excitation potential (columns 3 and 4) and the equivalent width of the line in the Sun observed in integrated light and in α Cen A and B (columns 7, 9, 11).

Fig. 1 shows a comparison between our equivalent width measurements for α Cen A and those of Furenlid & Meylan (1990). The slight systematic difference for the stronger lines comes probably from the use of different measurement techniques, our least squares fitting of Voigt profiles allowing a better modelling of the line wings.

4. Analysis

4.1. Solar gf-values

The two components of the α Cen system being rather similar to the Sun (especially α Cen A), the most accurate results are likely to be obtained via a strictly differential analysis with respect to the Sun.

However, because of bad weather conditions and a few instrumental problems, we could not observe the Sun in all the

windows in which we observed α Cen A and B. Thus, the solar gf-values were determined by fitting the lines measured in the Liège Solar Atlas, which concerns the disk center rather than the integrated light. The reliability of our results were checked by performing a differential analysis of the integrated Sun, as observed with the same instrument as the α Cen system, with respect to the Liège Solar Atlas. The final abundance results, however, are strictly differential since we subtract the abundances deduced from our integrated light solar spectra from the abundances deduced from our stellar spectra. The solar atlas is thus used only as an intermediate step.

For the Sun observed at the disk center, we adopt the semi-empirical model of Holweger and Müller (1974, HM) and the solar abundances of Grevesse et al. (1996). These abundances are given in Table 4 for our selected lines (column 2). Note that there is still some dispute about the precise value of the Fe abundance in the solar photosphere. We adopt the meteoretic value: $\log(N_{Fe}) = 7.51$, on a relative scale where $\log N_H = 12$, N_{Fe} and N_H being respectively the number densities of iron and hydrogen. Note that this choice has no effect on our differential abundances.

The solar gf-values and the solar equivalent widths measured at the disk center for all selected lines are listed in Table 4 (colunms 5 and 6).

4.2. Method

We adopt the classical method of analysis which consists, for each line, in adjusting the abundance until the calculated equivalent width is equal to the observed one.

In each star, the microturbulent velocity, ξ_t, is determined so that the abundances derived from the Fe I lines are independent of their equivalent widths.

The effective temperature T_{eff} is obtained by forcing the abundances derived from these Fe I lines to be independent of their excitation potential and the surface gravity by forcing the Fe II lines to indicate the same abundance as the Fe I lines.

The microturbulent velocity, the effective temperature, the gravity and the iron abundance are thus self-consitently determined in each star and, once the final model is obtained, the abundances of the other elements can be calculated.

4.3. Adopted models and physics

Our aim being to perform a strictly differential analysis of both components of the α Cen system relative to the Sun observed in integrated light, we interpolated the $T(\tau)$ relations for these three stars in the same grid of models, i.e. the ATLAS9 grid of Kurucz (1993). The opacities, the electron and gas pressures have then been computed from the temperature distribution by our own code, which makes use of the Gustafsson et al. (1975) routines for the calculation of the continuous absorption.

In the models, the iron abundance is taken as the metallicity indicator and the other heavy element abundances are scaled accordingly.

The line transfer calculations assume LTE and a plane parallel (horizontally homogeneous) atmosphere. The damping constant for the Van der Waals line broadening by hydrogen and helium atoms is calculated with the Unsöld formula (Gray 1976) with an empirical enhancement factor of 1.4 (Magain and Zhao 1996).

For the Sun observed in integrated light, the analysis with the theoretical model leads to $\log g = 4.44$ from the Fe ionization equilibrium and an effective temperature of 5780K from the excitation equilibrium of Fe I, in perfect agreement with the known values for the Sun.

The microturbulent velocity obtained with the theoretical model is slightly higher than the one obtained from the disk center spectra and the HM model: adopting $\xi_t = 0.9$ km/s in the latter case, we find $\xi_t = 1.06$ km/s for the Sun observed in integrated light. This slight difference may be due to anisotropies in the turbulence velocity field or to a variation of the microturbulent velocity with depth, but it may also come from a use of different solar models.

The derived Fe abundance is somewhat lower than that obtained with the HM model and the Sun observed at the disk center (Grevesse et al. 1996): 7.47 instead of 7.51. This discrepancy comes from the fact that the temperature of the theoretical model in the line-forming layers is slightly lower than that of the HM model.

In view of these comparisons, and of the fact that a few spectral regions could not be observed in integrated solar light, we adopted the following procedure for obtaining the most accurate relative abundances. For all lines, the gf-values were derived from the Liège solar atlas and the HM model. Then, the element abundances were determined in the two components of the α Cen system and in the Sun observed in integrated light with the same instrument, by using the theoretical models in all cases. The relative logarithmic abundances were then obtained as the differences between these abundance results.

5. Atmospheric parameters of α Cen A and B

The fundamental atmospheric parameters of the models derived for α Cen A and B are presented in Table 2, while Figs. 2 to 5 show the Fe abundance as a function of χ_{exc}, as obtained from Fe I lines in α Cen A and B.

We checked that, in each star, the microturbulent velocity and the effective temperature derived from Fe I are compatible with those derived from Ca I, Ti I, Cr I and Ni I. However, the Ca I, Ti I, Cr I and Ni I lines are fewer than the Fe I lines and do not span such a broad range of excitation potentials, thus leading to less accurate determinations.

As far as possible, the lines with equivalent width larger than 90 mÅ were rejected as they are more sensitive to damping than to microturbulence. We checked the influence of this equivalent width cutoff on the derived atmospheric parameters by repeating the analysis with Fe I lines having an equivalent width lower than 80,70,60 and 50 mÅ. The derived effective temperature and iron abundance don't change significantly in any of the two stars, remaining within the error bars given in Table 2.
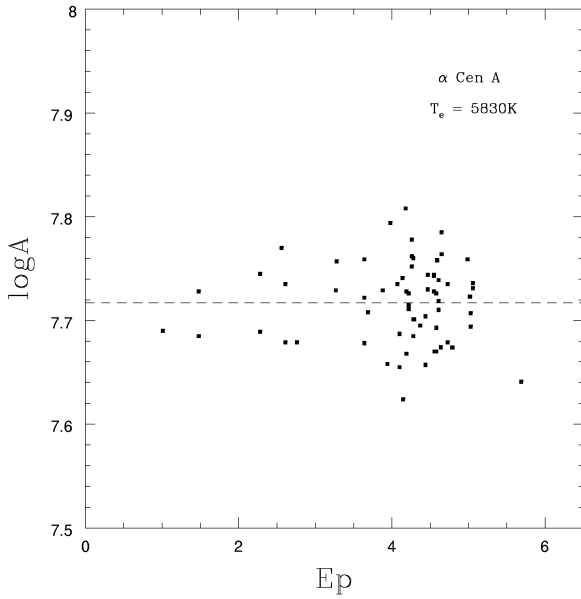
Fig. 2. Fe abundance as a function of χ_{exc}, as derived from Fe I lines in α Cen A. The dashed line is the regression line of the equivalent width against the excitation potential

Fig. 3. Fe abundance as a function of χ_{exc}, as derived from Fe I lines in α Cen B. The dashed line is the regression line of the equivalent width against the excitation potential

Table 2. Microturbulent velocity, ξ_t, effective temperature, T_{eff}, iron abundance with respect to the Sun, [Fe/H] = $\log(N_{\mathrm{Fe}}/N_{\mathrm{H}})_* - \log(N_{\mathrm{Fe}}/N_{\mathrm{H}})_\odot$ and logarithm of gravity, $\log g$ for α Cen A and B. The value of the solar abundance of iron, $\log(N_{\mathrm{Fe}}/N_{\mathrm{H}})_\odot$, is 7.47

	α Cen A	α Cen B
ξ_t (km/s)	1.09 ± 0.11	1.00 ± 0.08
T_{eff} (K)	5830 ± 30	5255 ± 50
[Fe/H]	0.25 ± 0.02	0.24 ± 0.03
$\log g$	4.34 ± 0.05	4.51 ± 0.08

The error bars for the microturbulent velocity correspond to 1σ statistical error on the slope of the linear regression in the abundance versus EW diagram. The error bars on the effective temperature account for the statistical error on the slope of the linear regression of the abundance versus excitation potential as well as for the uncertainty on the microturbulent velocity. The uncertainty on the iron abundance is obtained from the dispersion of the results around the mean and from the uncertainties on the microturbulent velocity and the effective temperature.

The gravities in α Cen A and B were first estimated with the classical formula:

$$\log(g/g_\odot) = \log(M/M_\odot) + 4\log(T_{\mathrm{eff}}/T_{\mathrm{eff},\odot}) - log(L/L_\odot)$$

In this formula, L and M are the luminosity and the mass of the star. With our solar model, our derived effective temperatures in α Cen A and B, $M_A/M_\odot = 1.085 \pm 0.01$, $M_B/M_\odot = 0.900$
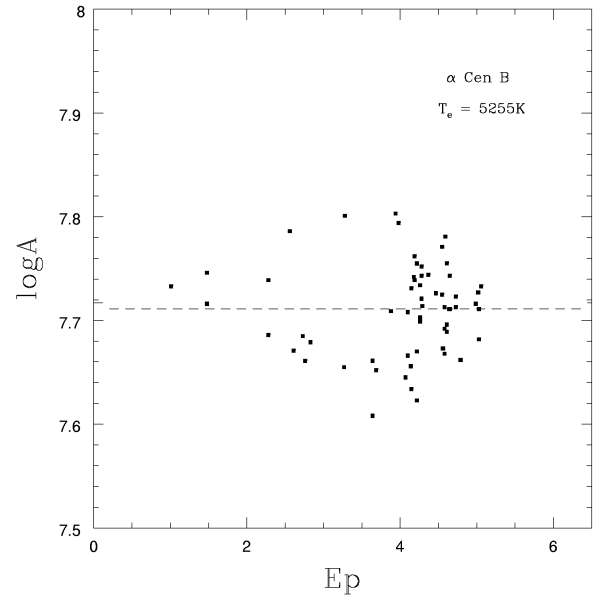
± 0.01, $log(L_A/L_\odot) = 0.1853 \pm 0.015$ and $log(L_B/L_\odot) = -0.3056 \pm 0.015$ (for references, see Noels et al. 1991), we find $\log g = 4.30 \pm 0.03$ in α Cen A and $\log g = 4.54 \pm 0.03$ in α Cen B.

The ionisation equilibrium of iron required $\log g = 4.34 \pm 0.05$ in α Cen A and $\log g = 4.51 \pm 0.08$ in α Cen B, the error bars being due to the dispersion of the abundance results derived from the Fe II lines. In both star, the spectroscopic and trigonometric values of the gravity are thus in agreement within the error bars.

Note that the 2.2 eV Fe I lines haven't been taken into account to derive the parameters of our models. As has been shown by Blackwell et al. (1984), they lead to a solar abundance which is significantly lower than indicated by the other Fe I lines. In our differential analysis, they lead to [Fe/H] = 0.24 ± 0.01 in α Cen A and 0.20 ± 0.01 in α Cen B, which indicates that, whatever the physical cause of this discrepancy, its effect is the same in α Cen A and may be reinforced in α Cen B, as compared with the Sun.

In α Cen A, our spectroscopically derived atmospheric parameters are in agreement with those of Chmielewski et al. (1992), although their effective temperature determination is based on the H_α line wings and the $T(\tau)$ laws from Eriksson et al. (for references, see Chmielewski et al., 1992). On the other hand, our effective temperature for α Cen B is clearly lower than theirs. Note that possible departures from LTE in the Fe I excitation equilibrium might affect the derived effective temperature of α Cen B (Edvardsson, private communication).

As a further check, we have also used the H_α line wings to determine the effective temperatures of α Cen A and B. Our H_α spectra were obtained under the same conditions as the ones
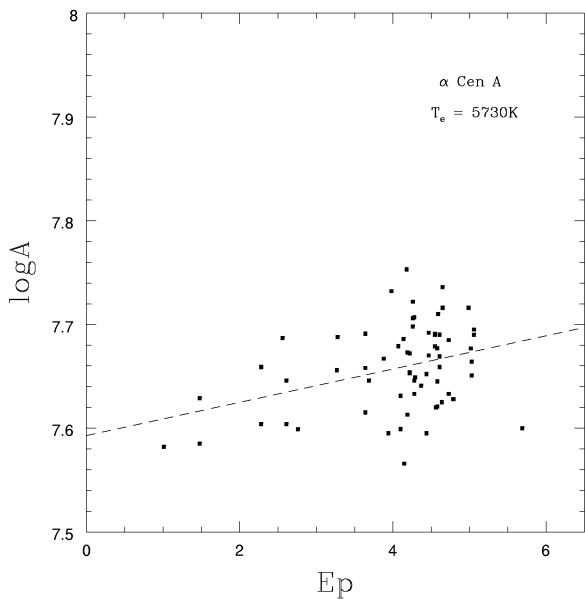
Fig. 4. Fe abundance as a function of χ_{exc}, as derived from Fe I lines in α Cen A. The effective temperature of the model is decreased by 100K. The dashed line is the regression line of the equivalent width against the excitation potential

Fig. 5. Fe abundance as a function of χ_{exc}, as derived from Fe I lines in α Cen B. The effective temperature of the model is increased by 100K. The dashed line is the regression line of the equivalent width against the excitation potential

used for the spectroscopic analysis of the metal lines. As it is not possible to determine accurately the position of the continuum in the vicinity of a line with very broad wings on the basis of CES spectra covering only a limited spectral region, we made a strictly differential analysis with respect to the Sun.

We did not attempt to determine the shape of the continuum in these spectral regions. Rather, we assumed that it is the same for the different objects observed and performed the analysis on the basis of the ratios of the (unnormalized) spectra - the unknow shape of the continuum cancelling in the ratio if it is the same for the different objects. We checked this stability by comparing the solar spectra obtained from the moonlight and from the light reflected by the 3.60m dome and found a perfect agreement.

In each star, the ratio between the stellar and the solar H_α profile obtained in the same observing conditions was compared with the ratio of theoretical H_α profiles (Kurucz, 1993) calculated for different stellar effective temperatures. Our observed ratios were normalised using two 'continuum' windows located rather far in the wings: $[6539.3 - 6540.3]$ Å and $[6590.2 - 6591.0]$ Å. The comparison between the observed and the theoretical ratios was then performed in two wavelength intervals located closer to the line center: $[6559.9 - 6560.2]$ Å and $[6566.3 - 6568.3]$ Å and led to $T_{eff,A} = 5820 \pm 15$ K and $T_{eff,B} = 5180 \pm 30$ K.

While the H_α temperature confirms the spectroscopic value for α Cen A, the value for α Cen B marginally disagrees with that derived from the excitation equilibrium of Fe I as well as with the value given by Chmielewski et al. (1992), which was determined
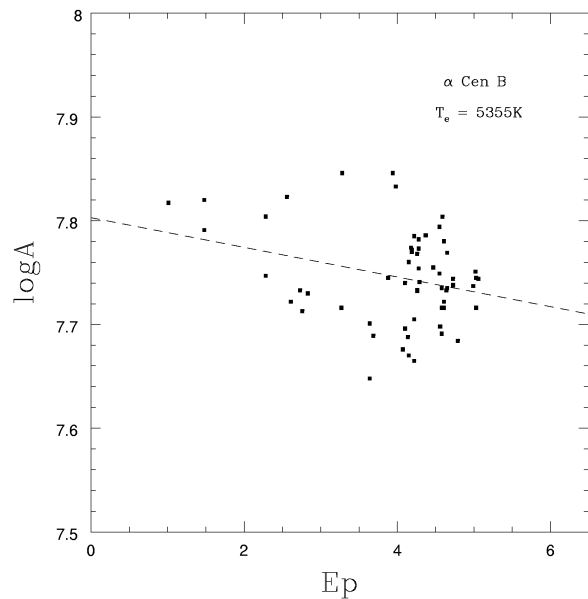
in a similar way, using similar data, but with different model atmospheres.

This discrepancy may be interpreted in the following way. The H_α line wings are formed in the upper parts of the convection zone, where the temperature distribution is sensitive to the adopted treatment of convection. Castelli et al. (1997) have shown that, in the Sun, the overshooting adopted in the ATLAS9 grids of Kurucz requires an effective temperature 100 - 150K higher than that of the Sun in order to fit the observed H_α profile.

In the two nearly identical stars α Cen A and the Sun, the errors are expected to cancel to first order and a strictly differential analysis remains valid.

That cancellation probably does not apply to the case of α Cen B, as the difference between the effective temperature derived from H_α profiles with models including or not the overshooting is smaller for cooler stars (Castelli et al., 1997). Comparing the ratio of the stellar and the solar H_α theoretical profile to the corresponding ratio of observed profiles thus leads to an underestimation of the effective temperature of α Cen B.

6. Element abundances

The abundances obtained for each line in the Sun and in α Cen A and B are presented in columns 8, 10 and 12 of Table 4. The mean values are given in Table 3. The 1σ error bars on the abundances in α Cen A and B result from the uncertainties on the effective temperature, the microturbulent velocity and the surface gravity, on the dispersion of the results around the mean and on the uncertainty of the solar abundance. This last uncertainty is determined from our spectra of the Sun observed

Table 3. Chemical abundances in the atmospheres of α Cen A and B. N_{el} and N_H are respectively the number density of the element considered and of Hydrogen. The first column gives the element, its atomic number Z, and the ionisation stage or molecular species from which the abundance of the element was derived, columns 2 and 3 give the solar abundances determined from observations at the disk center (Grevesse et al. 1996) and in integrated light, in a logarithmic scale where $\log N_H$ = 12. Columns 4 and 5 give the differential abundances in α Cen A and B with respect to the Sun: $[el/H]_* = \log\left(\frac{N_{el}}{N_H}\right)_* - \log\left(\frac{N_{el}}{N_H}\right)_\odot$

Element	$log\left(\frac{N_{el}}{N_H}\right)$	$\log\left(\frac{N_{el}}{N_H}\right)_\odot$	$[el/H]_A$	$[el/H]_B$
6 CI	8.55	8.54 ± 0.04	0.20 ± 0.05	0.28 ± 0.07
C$_2$	8.55	8.50 ± 0.04	0.20 ± 0.05	0.24 ± 0.04
7 N	7.97	7.96 ± 0.09	0.30 ± 0.09	—
8 OI	8.87	8.92 ± 0.03	0.21 ± 0.06	—
13 AlI	6.49	—	0.24 ± 0.04	0.24 ± 0.05
14 SiI	7.56	7.56 ± 0.02	0.27 ± 0.03	0.27 ± 0.04
20 CaI	6.35	6.34 ± 0.01	0.22 ± 0.03	0.21 ± 0.05
21 ScII	3.10	3.08 ± 0.04	0.25 ± 0.05	0.26 ± 0.04
22 TiI	4.93	4.85 ± 0.01	0.25 ± 0.03	0.27 ± 0.06
23 VI	4.02	3.92 ± 0.03	0.23 ± 0.05	0.32 ± 0.08
24 CrI	5.68	5.64 ± 0.01	0.24 ± 0.02	0.27 ± 0.04
24 CrII	5.68	5.64 ± 0.02	0.26 ± 0.03	0.26 ± 0.09
25 MnI	5.53	—	0.23 ± 0.04	0.26 ± 0.05
26 FeI	7.51	7.47 ± 0.01	0.25 ± 0.02	0.24 ± 0.03
26 FeII	7.51	7.47 ± 0.01	0.25 ± 0.02	0.25 ± 0.02
27 CoI	4.91	4.85 ± 0.02	0.28 ± 0.04	0.26 ± 0.04
28 NiI	6.25	6.24 ± 0.01	0.30 ± 0.03	0.30 ± 0.02
39 YII	2.23	2.16 ± 0.04	0.20 ± 0.05	0.14 ± 0.05
40 ZrII	2.61	2.48 ± 0.04	0.17 ± 0.05	—
63 EuII	0.54	0.56 ± 0.04	0.15 ± 0.05	0.14 ± 0.05

in integrated light and only accounts for the dispersion of the results around the mean.

In the calculation of the abundance of Fe from Fe I lines, the standard deviation of the results around the mean amounts to 0.04 dex (10 %). This value is thus taken as representative of the abundance uncertainty due to the EW uncertainties for the chemical elements for which only a single spectral line is available.

6.1. Even-Z elements: Si, Ca, Ti, Cr, Fe, Ni

Within the error bars, all these elements, except Ni, present the same overabundance (+0.24) with respect to the Sun. Moreover, in the two stars, the abundances of all these element coincide within the error bars. However, the Ni abundance seems to be some 15% higher than for the other even-Z elements.

6.2. Odd-Z elements: Al, Sc, V, Mn, Co

The lines of these elements are generally broadened by hyperfine structure, HFS. However, because of the lack of HFS data for most of the lines used in our analysis, the effect of HFS

was taken into account in an empirical way. First, the macroturbulent (+ rotation and instrumental) broadening was estimated by comparing the theoretical profiles of a few Fe I lines with the observations. The total broadening velocities were found respectively at 1.7, 3.1, 3.5, and 2.3 km/s for the Sun observed at disk center, for the Sun observed in integrated light and for α Cen A and B. Then, for each line affected by HFS, we determined the number of HFS components and the splittings so as to reproduce the observed line width and profile in the solar spectrum. We checked that our empirical model also leads to satisfactory fits in the Sun observed in integrated light and in α Cen A and B.

The abundances of these elements in α Cen A and B agree within the error bars. In contrast with Furenlid and Meylan (1990), we find no difference in the odd/even effect in the α Cen system, as compared to the Sun and, thus, no evidence for an enrichment of the prestellar medium by the ejecta of a Type II supernova (the differential odd-even effect amounts to 0.00 ± 0.01 in α Cen A and 0.02 ± 0.02 in α Cen B).

6.3. Neutron capture elements: Y, Zr, Eu

Only one good line was available for each of these elements. The HFS structure and the isotopic shift of the Eu II line were taken into account following Biehl (1976).

These neutron capture elements are less overabundant than iron and all lighter elements.

6.4. C N O

Carbon

The carbon abundance has been derived from the λ 5380.320 Å C I line and the λ 5143.342 Å C$_2$ line. In α Cen A, these two lines lead to the same differential abundance. Note that the C I line is highly excited (7.68 eV), while the excitation potential of the C$_2$ line is much lower: 0.10 eV; therefore, these lines are formed in rather different atmospheric layers. In α Cen B, the abundance derived from the highly excited C I line tends to depart from that derived from the C$_2$ line and from the values found in α Cen A, altough it still remains compatible when the error bars are taken into account.

We considered other highly excited lines, at λ 6587.620, 6671.820, 6674.199, 6679.580 and 7476.176 Å but as these lines seem to be perturbed by small blends, there were rejected from the final analysis.

Nitrogen

Three CN lines have been used to derive the abundance of nitrogen in the Sun observed in integrated light and in α Cen A. Many CN lines appear in the spectral window centered on 8210Å, but, since most of them overlap, their EWs were found to be much less reliable and we decided to drop them. Moreover, in α Cen B, all the CN lines were too much perturbed to lead to accurate

abundances. The abundance of nitrogen has been calculated using the mean carbon abundance given by C I and C_2, i.e. 8.52 in the Sun observed in integrated light and 8.72 in α Cen A.

We found a rather large scatter between the abundances indicated by the three CN lines reported in Table 4. However, the deviations are very similar in the Sun and in α Cen A, so that the error on the mean abundance is strongly reduced (from 0.13 to 0.05 dex) when making a line-by-line differential analysis. As we do not know the cause of this scatter, we adopt an error bar which is in between these two extremes.

Oxygen

In the spectra of the Sun observed in integrated light, only two highly excited O I lines (10.74 eV), at λ 6156.80 and 6158.17Å were available. The mean abundance indicated by these two lines is 8.92 ± 0.03.

The forbidden O I line at 6300.31Å is blended by a Ni I line which is clearly visible in the spectra of α Cen A and B. Lambert (1978) estimated the maximum EW of this Ni I line to be 0.5 mÅ in the Sun observed at disk center. We used this estimate to calculate its solar $\log gf$, as well as that of the remaining [O I] line. In α Cen A and B, the EW of the Ni I blend has been calculated with the Ni abundance derived from the other Ni I lines, and amounts respectively to 1.1 and 1.4 mÅ. Table 4 gives the total EW of the blended [O I] line, but the abundances are computed taking the blend into account.

In α Cen A, the two highly excited lines lead to the following abundances: 9.16 and 9.07 respectively, in agreement with the value of 9.14 indicated by the forbidden line. The mean abundance derived from the three lines is thus 9.12 ± 0.06.

In α Cen B, the forbidden line leads to an oxygen abundance of 9.19, compatible with the value found in α Cen A. The only excited line that could be measured is the line at λ 6156.80Å. It leads to an oxygen abundance of 9.69, three times larger than in α Cen A. Because of the discrepancy between the two lines, we could not derive a reliable oxygen abundance in α Cen B.

The cause of this discrepancy between the low excitation line, which is formed in rather high layers, and the high excitation one, which originates from much deeper layers, may be related to the discrepancy between the effective temperatures deduced from the Fe I excitation equilibrium on the one hand and from the H_α line wings on the other hand. As the high excitation line is likely to originate from the top of the convection zone, the treatment of convective transport in the Kurucz models may, once more, be responsible for the observed mismatch. Moreover, in solar-type stars, non-LTE effects have been found to affect the high excitation O I lines (Kiselman, 1991) and temperature inhomogeneities to affect both the forbidden and the high excitation O I lines (Kiselman & Nordlund, 1995). The errors in the two similar stars, α Cen A and the Sun, probably cancel to first order, but this is not the case for the cooler α Cen B.

7. Conclusions

The discrepancies affecting the previous determinations of the effective temperature and the metallicity of α Cen A and B prompted us to repeat the analysis of these important objects, using the best possible data as well as a very careful and self-consistent spectroscopic analysis. The two stars being solar-like, the analysis was performed differentially with respect to the Sun. The 3 stars were observed at La Silla, Chile, in may 1993 and 33 spectral regions were covered. In each region, the S/N ration reaches 550. The data reductions used special procedures written in the ESO-MIDAS environnement.

In α Cen A, the effective temperature is derived from the excitation equilibrium of neutral Fe and is in agreement with that obtained from the H_α line wings. The spectroscopic parameters of α Cen A are in agreement with those derived by Chmielewski et al. (1992), although they used different models. In α Cen B, the two techniques lead to marginally discrepant results, due to the sensitivity of the H_α line wings to the treatment of convection. This effect does not appear in α Cen A, which is more solar-like: in this star, the differential analysis cancels out the model dependency of the H_α method.

The abundance determinations have been performed for a restricted number of elements, since we decided to keep only the lines of sufficient quality. In the two stars, the element abundances coincide within the error bars, showing thus no evidence of enhanced helium diffusion processes in α Cen B.

The even-Z elements present the same overabundance as iron, with respect to the Sun, except Ni, which seems more overabundant.

When the HFS structure of the odd-Z elements is taken into account, no enhanced odd/even effect is found in the α Cen system, as compared to the Sun. This is in contradiction with the results of Furenlid and Meylan (1990), and shows no evidence for a SN II progenitor for the α Cen system.

The clearest departure from solar relative abundances lies in the less pronounced enhancement of the neutron capture elements, for the ones synthesized by the s-process as well as for the r-process products. The nucleosynthetic interpretation of this effect does not appear obvious as the r and s elements are generally thought to be produced in quite different astrophysical environments.

A attempt has also been made to derive the CNO abundances. The uncertainties are generally larger than for the heavier elements, and do not reveal any significant difference when compared to Fe.

References

Abia C., Rebolo R., Beckman J.E., Crivellari L., 1988, A&A 206, 100

Bessell M.S., 1981, Proc. Astron. Soc. Australia 4, 212

Biehl D., 1976, "Bestimmung der Hyperfeinstruktur astrophysikalisch interessanter Niveaus und Spektrallinien schwerer Elemente",Christian-Albrechts-Universitat, Kiel, Institut fur Theoretische Physik und Sternwarte.

Blackwell D.E., Booth A.J., Petford A.D., 1984, A&A 132, 236

Böhm-Vitense E., 1958, Zt. Ap. 46, 108.

Castelli F., Gratton R.G., Kurucz R.L., 1997, A&A 318, 841

Chmielewski Y., Friel E., Cayrel de Strobel G., Bentolila C., 1992, A&A 263, 219

Delbouille L., Roland G., Neven L., 1973, "Atlas photosphérique du spectre solaire de 3000 à 10000 Å", Institut d'Astrophysique de l'Université de Liège

Demarque, P., Guenther, D.B., van Altena, W.F., 1986, Astrophys. J. 300, 773

Drayson S.R., 1975, J. Quant. Spectosc. Radiat. Transfer 16, 611

Edvardsson B., 1988, A&A 190, 148

Edvardsson B., Andersen J., Gustafsson B., Lambert D.L., Nissen P.E., Tomkin J., 1993, A&A 275, 101

England M.N., 1980, MNRAS 191, 23

Fernandes J., Neuforge C., 1995, A&A 295, 678

French U.L., Powell A.T.L., 1971, Royal Obs. Bull. 173, 63

Furenlid I., Meylan T., 1990, Ap. J. 350, 827

Gray D. F., "The Observation and Analysis of Stellar Photosphere", 1976, eds. Wiley-Interscience.

Grevesse N., Noels A., Sauval J., 1996, "Cosmic Abundances", Eds. Holt S.S., Sonneborn G., ASP Conference Series, vol 99, pp. 117

Gustafsson B., Bell R.A., Erikson K., Nordlund Å, 1975, A&A 42, 407

Holweger H., Müller E.A., 1974, Solar Physics 39, 19

Kiselman D., 1991, A&A 245, L9

Kiselman D., Nordlund Å, 1995, A&A 302, 578

Lambert D. L., 1978, MNRAS 182, 249

Meylan T., Furenlid I., Meylan P., 1992, BAAS 23, 1384

Kurucz R. L., Peytremann E. 1975, SAO Special Report 162

Kurucz R. L., 1993, ATLAS9 Stellar Atmosphere Programs and 2kms^{-1} grid, Kurucz CD-ROM No. 13

Magain P., Zhao G., 1996, A&A 305, 245

Neuforge C., Christensen-Dalsgaard J., Chaboyer B., Noels A, 1997, in press

Noels, A., Grevesse, N., Magain, P., Neuforge, C., Baglin, A., Lebreton, Y. 1991, Astron. Astrophys 247, 91.

Press W.H., Teukolsky S.A., Vettering W.T., Flannery B.P. 1990, "Numerical Recipes", Cambridge University Press.

Smith G., Edvardsson B., Frisk U., 1986, A&A 165, 126.

Soderblom D.R., 1986, A&A 158, 273.